

Uni-RS: A Spatially Faithful Unified Understanding and Generation Model for Remote Sensing

Weiyu Zhang^{1,†}, Yuan Hu^{1,†}, Yong Li^{1,2} and Yu Liu^{1,*}

¹Institute of Remote Sensing and Geographic Information System, School of Earth and Space Sciences, Peking University, Beijing, 100871, China

²Department of Civil and Environmental Engineering, The Hong Kong University of Science and Technology, Hong Kong ^{*†}

{weiyu_zhang, huyuan}@pku.edu.cn, yong.li@connect.ust.hk, liuyu@urban.pku.edu.cn

Abstract

Unified remote sensing multimodal models exhibit a pronounced spatial reversal curse: although they can accurately recognize and describe object locations in images, they often fail to faithfully execute the same spatial relations during text-to-image generation, where such relations constitute core semantic information in remote sensing. Motivated by this observation, we propose Uni-RS, the first unified multimodal model tailored for remote sensing, to explicitly address the spatial asymmetry between understanding and generation. Specifically, we first introduce explicit Spatial-Layout Planning to transform textual instructions into spatial layout plans, decoupling geometric planning from visual synthesis. We then impose Spatial-Aware Query Supervision to bias learnable queries toward spatial relations explicitly specified in the instruction. Finally, we develop Image–Caption Spatial Layout Variation to expose the model to systematic geometry-consistent spatial transformations. Extensive experiments across multiple benchmarks show that our approach substantially improves spatial faithfulness in text-to-image generation, while maintaining strong performance on multimodal understanding tasks like image captioning, visual grounding, and VQA tasks.

1 Introduction

The evolution of Multimodal Large Language Models (MLLMs) is shifting from perception-centric architectures towards unified frameworks capable of both understanding and generation [Zhang *et al.*, 2025]. In the context of Remote Sensing (RS), this shift is particularly transformative. A unified model can serve as a generative simulator [Yang *et al.*, 2025; Liu *et al.*, 2025a], synthesizing samples for data-scarce scenarios (e.g., disaster aftermaths), while facilitating language-driven image editing (e.g., removing cloud artifacts). While unified multimodal understanding and generation have been widely explored in general domains [Team,

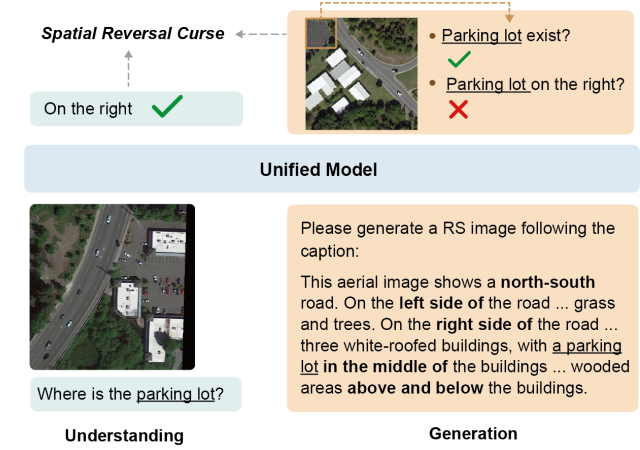


Figure 1: Illustration of the Spatial Reversal Curse in unified remote sensing multimodal models. While the model correctly describes spatial relations from an input image (left), it often fails to faithfully execute the same relations during text-to-image generation (right).

2024; Xie *et al.*, 2025; Pan *et al.*, 2025], to the best of our knowledge, such a unified framework has not yet been studied in the field of remote sensing.

However, adapting unified models to the RS domain presents unique challenges. Unlike natural images typically centered on salient objects, RS imagery is characterized by a “bird’s-eye view” [Xia *et al.*, 2018], featuring high object density and intricate spatial layouts, where spatial relations are as semantically critical as the objects themselves. When standard unified models are directly adapted to the remote sensing domain, a critical limitation emerges. Similar to the well-documented *Reversal Curse* [Berglund *et al.*, 2024] in large language models—where knowledge acquired in one direction does not reliably transfer to its inverse—we observe an analogous phenomenon in remote sensing unified models. Specifically, models can accurately recognize and describe spatial layouts from images, yet fail to faithfully reproduce the same layouts during text-to-image generation (Figure 1). We term this systematic asymmetry the *Spatial Reversal Curse*. For instance, a model that correctly identifies “a stadium next to a river” from image may generate the two objects far apart given this caption. This disconnect in-

* Corresponding author.

† Equal contribution.

dicates that spatial knowledge is encoded for perception but misaligned for generation.

We attribute this capability gap to how spatial information is introduced and passed through along the generation pathway. First, spatial relations are typically expressed implicitly and sparsely in language and are easily dominated by object-centric descriptions during generation. In remote sensing imagery, dense object layouts make accurate modeling of spatial relations especially important for correct scene understanding and generation, thereby amplifying the impact of this limitation. Second, in unified architectures that interface large language models with diffusion-based image generators, textual instructions are mapped into a compact conditioning representation prior to image synthesis. During this process, abstract and relational information—such as spatial layout—is more fragile than appearance-related cues and is therefore more susceptible to attenuation.

To address this gap, we propose Uni-RS, a unified multimodal model tailored for remote sensing imagery. Uni-RS incorporates three complementary design choices to improve spatial faithfulness during generation. First, Spatial-Layout Planning addresses the tendency of spatial constraints to be overshadowed by object-centric descriptions by reformulating textual instructions into structured layout plans that make spatial information more salient. Second, Spatial-Aware Query Supervision mitigates the loss of spatial information in the pathway from MLLM to diffusion model by explicitly supervising a subset of learnable queries to encode spatial relations in the instruction. Third, we introduce Image–Caption Spatial Layout Variation, a rotation-based data construction strategy that improves spatial adherence by training the model on the same objects arranged under different spatial layouts.

To summarize, our main contributions are threefold:

- We identify and systematically characterize the Spatial Reversal Curse in unified remote sensing models.
- We present Uni-RS, the first unified remote sensing multimodal model and improves its spatial faithfulness in image generation.
- The proposed Uni-RS achieves consistent improvements in spatially faithful image generation while maintaining strong multimodal understanding performance.
- We construct RS-Spatial, a large-scale spatial annotation dataset that enhances spatial faithfulness in unified model training.

2 Related Work

2.1 Unified Understanding and Generation

Recent research has significantly advanced unified multimodal models capable of both image understanding and generation. Existing approaches can be broadly categorized into three paradigms. The first follows an autoregressive (AR) formulation, modeling both vision and language as a unified sequence within a single large language model (LLM) [Team, 2024; Wang *et al.*, 2024; Chen *et al.*, 2025b]. The second paradigm also leverages a single MLLM for understanding and generation, but adopts a diffusion-based strategy for image synthesis [Zhou *et al.*, 2024; Liang *et al.*, 2025;

Xie *et al.*, 2025]. The third paradigm combines pretrained MLLMs with diffusion models by assigning semantic reasoning to the MLLM and delegating high-fidelity image generation to the diffusion component [Pan *et al.*, 2025; Wu *et al.*, 2025; Chen *et al.*, 2025a]. Our approach falls into this third paradigm, extending it to a unified remote sensing setting with explicit spatial modeling.

2.2 Unified Understanding and Generation in RS

While unified understanding and generation have been extensively studied in general-domain vision–language models, research in the remote sensing (RS) community has largely followed decoupled trajectories. On the understanding side, recent years have witnessed the emergence of RS MLLM, beginning with RSGPT [Hu *et al.*, 2025] and followed by instruction-tuned systems such as SkySenseGPT [Luo *et al.*, 2024], GeoChat [Kuckreja *et al.*, 2024], GeoLLaVA-8K [Wang *et al.*, 2025b], and EarthGPT [Zhang *et al.*, 2024a]. In parallel, remote sensing image generation has progressed from early GAN-based approaches such as StrucGAN [Zhao and Shi, 2021] to diffusion-based generative models including DiffusionSat [Khanna *et al.*, 2024], CRS-Diff [Tang *et al.*, 2024], Text2Earth [Liu *et al.*, 2025a], and MetaEarth [Yu *et al.*, 2024]. Despite these advances, multimodal understanding and image generation in RS have largely been studied in isolation, and a unified framework that jointly supports understanding and faithful image generation remains underexplored.

2.3 Spatial Planning in Vision–Language Models

Chain-of-Thought (CoT) prompting [Wei *et al.*, 2022] and its multimodal extensions [Zhang *et al.*, 2024b; Liu *et al.*, 2023] have been widely adopted to elicit step-by-step reasoning in vision–language models, enabling more interpretable decision-making and complex task decomposition. In RS domain, CoT-based supervised fine-tuning has further been explored to inject structured geographic reasoning into RS-VLMs, including approaches such as GeoChain [Yeramilli *et al.*, 2025], GeoSpatial CoT [Liu *et al.*, 2025b], GeoZero [Wang *et al.*, 2025a], and GeoReason [Li *et al.*, 2026], as well as recent reasoning-centric models trained on large-scale RS reasoning datasets [Köksal and Alatan, 2025; Fiaz *et al.*, 2025; Li *et al.*, 2025]. However, these methods primarily focus on producing or supervising explicit reasoning traces for understanding tasks, rather than externalizing spatial layout information in a form that can directly guide image generation. In contrast, our work emphasizes spatial planning over reasoning explanation, aiming to make object layouts and spatial constraints explicit for faithful text-to-image synthesis.

3 Characterizing the Spatial Reversal Curse

While unified MLLMs have demonstrated strong performance in general vision–language domains, their transfer to RS imagery exposes a non-trivial discrepancy. When adapting the unified model to RS data, we observe the Spatial Reversal Curse between spatial understanding and image generation: Although the model can accurately recognize spatial

relations in the understanding direction, it often fails to faithfully execute the same relations in the generation direction.

Crucially, this discrepancy cannot be explained by object hallucination or low visual fidelity, as the target objects are often correctly synthesized but misplaced. To determine whether this phenomenon reflects isolated failure cases or a fundamental limitation of unified RS models, we move beyond qualitative examples and conduct a controlled quantitative characterization.

3.1 A Symmetric Evaluation Protocol for Spatial Consistency

To rigorously characterize the asymmetry between spatial understanding and spatial generation, we design a paired and symmetric evaluation protocol. We adopt RSIEval [Hu *et al.*, 2025] as our testbed due to its suitability for spatial analysis, which provides high-resolution imagery with expert-annotated captions explicitly describe spatial layouts and object positions.

To isolate the model’s ability to associate a single object with its explicit spatial location, we restrict our evaluation to unary spatial relations and adopt a standardized 3×3 grid as a shared spatial reference system for both understanding and generation tasks. The evaluation set is constructed through a model-assisted, human-verified pipeline, yielding 126 high-quality samples with unambiguous object–location annotations (details in Appendix).

We define complementary metrics to quantify this asymmetry. For spatial understanding, we formulate the task as a nine-way classification problem. Given an image I and the query “Where is the object located?”, the model is required to predict the correct grid cell. We report Spatial Understanding Accuracy (SUA), defined as:

$$\text{SUA} = \frac{1}{N} \sum_{i=1}^N \mathbb{1}(\hat{L}_i = L_{gt}^{(i)}) \quad (1)$$

where \hat{L}_i and $L_{gt}^{(i)}$ denote the predicted and ground-truth locations for the i -th sample, respectively.

For image generation, we evaluate spatial faithfulness using two hierarchical metrics. The first is Object Generation Rate (OGR), which measures whether the model successfully synthesizes the target object, regardless of its spatial placement:

$$\text{OGR} = \frac{1}{N} \sum_{i=1}^N \mathbb{1}(E_i = 1), \quad (2)$$

where $E_i = 1$ indicates that the target object is correctly detected in the generated image. OGR serves as an upper bound on spatial performance, as correct spatial placement is impossible if the object itself is missing.

The second metric is Spatially Faithful Rate (SFR), which measures the joint probability that the target object is both generated and placed in the correct spatial region specified by the prompt:

$$\text{SFR} = \frac{1}{N} \sum_{i=1}^N \mathbb{1}(E_i = 1 \wedge P_i = 1), \quad (3)$$

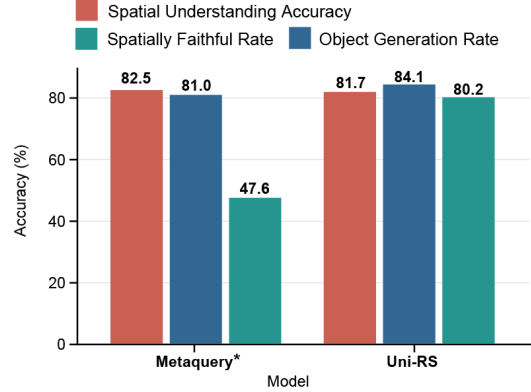


Figure 2: Quantitative characterization of the Spatial Reversal Curse. The baseline MetaQuery* model exhibits a pronounced gap between spatial understanding and spatially faithful text-to-image generation. The * denotes that the model was trained by us under the same experimental settings as described in Section 5.1 due to the absence of public checkpoints. The Uni-RS largely reduces this gap after incorporating the proposed spatial mechanisms.

where $P_i = 1$ denotes correct placement in the ground-truth grid cell.

3.2 Findings

We tested the Spatial Reversal Curse using MetaQuery. As no public checkpoint is available, we train MetaQuery using the official implementation under the same experimental settings described in Section 5.1. As shown in Figure 2, MetaQuery achieves a high Spatial Understanding Accuracy (SUA) of 82.54%, which indicates that the model possesses sufficient perceptual capacity to recognize spatial layouts from remote sensing imagery in the understanding direction.

In contrast, when conditioned on equivalent textual instructions for text-to-image generation, the same model exhibits a pronounced degradation in spatial faithfulness. Although the target object is frequently synthesized, with an Object Generation Rate (OGR) of 80.95%, correct spatial placement is achieved in less than half of the cases, as reflected by a Spatially Faithful Rate (SFR) of 47.61%.

The discrepancy yields a substantial spatial gap of

$$\Delta = \text{OGR} - \text{SFR} = 33.34\%,$$

indicating that generation failures predominantly stem from incorrect spatial execution rather than object hallucination or missing content. In other words, even when the model successfully synthesizes the target object, it frequently fails to place it in the intended spatial region specified by the instruction.

To further examine the generality of this phenomenon beyond the MetaQuery-style paradigm, we additionally experiment with Show-o [Xie *et al.*, 2025]. After fine-tuning Show-o on remote sensing data, we observe a similar asymmetry, where Δ achieves 27.8. Detailed experimental settings and results for Show-o are provided in the Appendix.

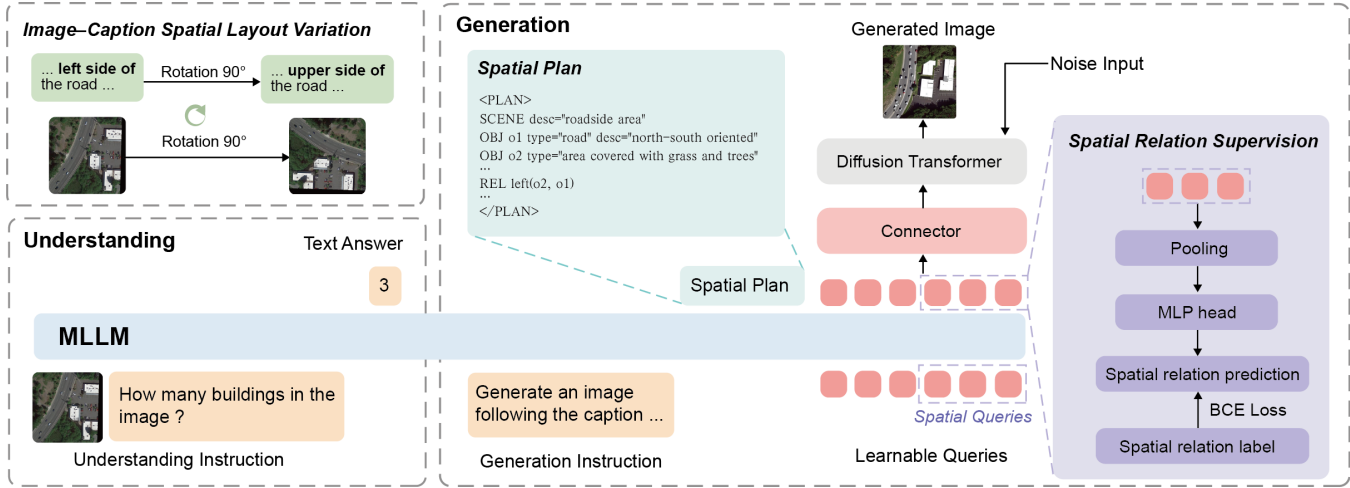


Figure 3: Overview of the Uni-RS framework. Uni-RS integrates a multimodal large language model (MLLM) with a diffusion-based image generator through learnable queries and a Transformer-based connector. During training, the framework is further enhanced by Spatial-Layout Planning, Spatial-Aware Query Supervision, and geometry-consistent image–caption transformations, which jointly reinforce instruction-level spatial constraints and improve spatial faithfulness during generation.

4 Methodology

4.1 Model Architecture

We adopt a unified framework that bridges a multimodal large language model (MLLM) and a diffusion-based image generator through a set of learnable queries. As illustrated in Fig. 3, textual instructions are first processed by the MLLM, and the resulting query representations are transformed into conditioning signals that guide diffusion-based image synthesis. We adopt Qwen2.5-VL-3B [Bai *et al.*, 2025b] as the multimodal large language model backbone and SANA-1.6B [Xie *et al.*, 2024] as the diffusion-based image generator, bridged by $N = 256$ learnable queries and a 24-layer Transformer-based connector. This configuration follows the best practice of MetaQuery [Pan *et al.*, 2025] and is fixed across all experiments.

Within this unified framework, Uni-RS incorporates three complementary spatial mechanisms. First, during text-to-image generation, the MLLM produces an explicit *spatial plan* from the input textual instruction, which is attended by learnable queries to pass through the spatial layout plan to diffusion-based synthesis. Second, a subset of the learnable queries is designated as *spatial queries* and supervised with spatial relation labels via an auxiliary prediction head, providing explicit spatial relation signals that regularize the conditioning interface between the MLLM and the diffusion model. Third, Uni-RS adopts image–caption spatial layout variation, in which geometrically transformed image–caption pairs are used during training to expose the unified framework to systematic changes in object locations and spatial relations. We next describe each of these components in detail.

4.2 Spatial-Layout Planning

Remote sensing image generation often involves complex scenes with dense object distributions. In such cases, spatial layout constraints are easily overshadowed by long, object-

centric descriptions, as object names correspond to salient visual patterns, whereas spatial relations are abstract and implicit supervised by standard generative objectives.

To make spatial constraints explicit, we introduce Spatial-Layout Planning. Although Spatial-Layout Planning produces an auxiliary textual plan, its purpose differs fundamentally from chain-of-thought prompting: rather than explaining reasoning steps, the plan explicitly externalizes spatial layout information that is otherwise implicit in natural language instructions. Concretely, Spatial Planning rewrites a user instruction into a structured layout specification expressed in text. Instead of relying on raw captions alone, the MLLM generates a plan enclosed by a `<plan>` tag, which specifies the global scene context (SCENE), instantiates object instances with coarse spatial locations (OBJ), and enumerates explicitly stated spatial relations (REL), as shown in Figure 3

Importantly, Spatial-Layout Planning rewrites the instruction into a spatially explicit textual plan that makes object instances, coarse locations, and spatial relations salient. By restructuring how spatial information is expressed in language, this plan encourages the conditioning learnable queries to better preserve the intended spatial constraints during image generation.

4.3 Spatial-Aware Query Supervision

The learnable queries serve as the primary carriers of conditioning information passed from the MLLM to the diffusion model. When rich language instructions are compressed into a fixed set of queries, fine-grained spatial cues may be attenuated. To mitigate this effect, we introduce a spatial-aware query supervision term: during training, a subset of queries, denoted as $Q_{spa} \subset Q$, is softly biased to retain spatial relations that are explicitly mentioned in the instruction via an auxiliary supervision signal.

This supervision relies on a closed-set vocabulary of spatial relations that reflects how spatial concepts are expressed

in remote sensing captions. Drawing on cognitive geography, we organize spatial expressions into five broad categories: directional, topological, distance-based, orientation-based, and distributional relations, with the last capturing characteristic multi-object arrangements in overhead imagery. Based on this taxonomy, we construct a spatial relation vocabulary \mathcal{V} with $K = 79$ spatial relation labels, which provides coverage of spatial expressions appearing in the training corpus (See details of the spatial relation vocabulary in Appendix).

Given an instruction, we extract the spatial relations it explicitly mentions to obtain a multi-hot target vector $\mathbf{y} \in \{0, 1\}^K$. During training, features from \mathbf{Q}_{spa} are aggregated (e.g., via mean pooling) and passed through a lightweight projection head to predict $\hat{\mathbf{y}} \in \mathbb{R}^K$:

$$\hat{\mathbf{y}} = \sigma(\text{MLP}(\text{Pool}(\mathbf{Q}_{\text{spa}}))). \quad (4)$$

We supervise this prediction using a binary cross-entropy loss:

$$\mathcal{L}_{\text{spa}} = \text{BCE}(\hat{\mathbf{y}}, \mathbf{y}). \quad (5)$$

This auxiliary loss biases the spatial-aware queries to preserve instruction-level spatial cues that are subsequently reflected in the conditioning signals used for image generation. In our experiments, we designate the last 32 queries as \mathbf{Q}_{spa} , providing sufficient capacity to encode spatial relations, while preserving the remaining queries for modeling object semantics and other non-spatial information.

4.4 Image–Caption Spatial Layout Variation

Finally, we introduce Image–Caption Spatial Layout Variation as a geometry-aware training strategy. This design exploits a geometric property of overhead imagery: rotating a remote sensing image preserves scene semantics, object categories and attributes, as well as topological, distance-based, and distributional spatial relations, while resulting in systematic changes to absolute object locations and orientation- or direction-dependent spatial relations.

Concretely, for each training image, we generate rotated variants with angles $\theta \in \{90^\circ, 180^\circ, 270^\circ\}$. To maintain geometric consistency between vision and language, the associated caption is rewritten accordingly. Given a rotation angle θ , a large language model is prompted to identify spatial expressions in the original caption and update those that are direction- or orientation-dependent based on the corresponding geometric transformation (e.g., changing “North of” to “East of” for a 90° clockwise rotation), while preserving scene descriptions, object categories, attributes, and rotation-invariant spatial relations. The rewritten caption remains linguistically fluent and semantically aligned with the rotated image.

As a result, the training data contain paired image–caption instances that depict identical scenes and objects but differ in absolute object locations and orientation-sensitive spatial relations. This paired variation isolates spatial layout changes, enabling the model to associate spatial-related descriptions with geometric transformations instead of memorizing absolute object locations.

Table 1: Comparison with existing text-to-image generation methods on RSICD. \dagger indicates methods evaluated without fine-tuning on RSICD. See Supplementary Materials for detailed descriptions of baselines.

Method	FID (\downarrow)	Zero-Shot Cls-OA (\uparrow)	CLIP (\uparrow)
Attn-GAN	95.81	32.56%	20.19
DAE-GAN	93.15	29.74%	19.69
DF-GAN	109.41	51.99%	19.76
Lafite	74.11	49.37%	22.52
DALL-E	191.93	28.59%	20.13
Txt2Img-MHNvQVAE	175.36	41.46%	21.35
Txt2Img-MHNvQGAN	102.44	65.72%	20.27
RSDiff	66.49	—	—
CRS-Diff	50.72	69.31%	20.33
Text2Earth †	67.92	—	23.91
Text2Earth	24.49	90.26%	25.62
Uni-RS (Ours) †	46.83	66.93%	24.11
Uni-RS (Ours)	22.11	91.63%	25.68

Table 2: Comparison of spatial fidelity and generation quality on RSIEval and VRSBench. \dagger indicates methods evaluated without fine-tuning on the corresponding dataset.

Method	RSIEval			VRSBench	
	FID (\downarrow)	SFR (\uparrow)	CLIP (\uparrow)	FID (\downarrow)	CLIP (\uparrow)
Text2Earth †	17.07	63.40	0.2374	8.28	0.2485
Text2Earth	16.22	65.10	0.2379	7.42	0.2493
Uni-RS (Ours)	13.04	80.15	0.2401	4.51	0.2546

4.5 RS-Spatial: A Spatial Annotation Dataset for Training Uni-RS

To support the proposed spatial mechanisms in a unified and systematic manner, we construct a new large-scale spatial annotation dataset, termed RS-Spatial, built upon RSICap [Hu *et al.*, 2025] and VRSBench [Li *et al.*, 2024]. This dataset aims to provide additional spatial layout supervision for remote sensing text-to-image generation in unified models.

RS-Spatial contains three types of spatial annotations: (i) structured layout descriptions for Spatial-Layout Planning, (ii) spatial relation labels aligned with the predefined vocabulary for spatial-aware query supervision, and (iii) rewritten captions corresponding to rotated images for image–caption spatial layout variation. All annotations are generated using Qwen3-VL-235B-A22B-Instruct [Bai *et al.*, 2025a] through a shared two-stage pipeline. In the first stage, the model is prompted to produce task-specific annotations for each image–caption pair. In the second stage, the same model verifies the consistency between the generated annotations and the original image–caption pairs or applied rotations, and samples that fail this verification are discarded. In total, RS-Spatial contains 20,496 structured spatial layout plans, 22,849 spatial relation annotations, and 36,702 rotation-consistent image–caption pairs.

Importantly, RS-Spatial introduces no new semantic content beyond what is explicitly supported by the original cap-

Table 3: Unified comparison on RSIEval and VRSBench-val across multimodal understanding tasks. \dagger indicates methods evaluated without task-specific fine-tuning.

RSIEval						VRSBench-val							
Method	Captioning				VQA	Method	Captioning				VQA	Grounding	
	B-4	METEOR	R-L	CIDEr	Avg		B-4	METEOR	R-L	CIDEr	Avg	Acc@0.5	Acc@0.7
BLIP2	0.01	3.40	11.57	0.09	45.56	Mini-Gemini	14.3	21.5	36.8	33.5	77.8	30.1	6.8
MiniGPT4	17.26	19.87	35.32	16.25	21.82	GeoChat	13.8	21.1	35.2	28.2	76.0	49.8	19.9
RSGPT	22.07	23.58	41.73	31.35	65.24	GeoPix	14.0	23.4	36.3	31.3	74.9	49.8	20.0
GeoPix \dagger	2.76	9.36	16.12	2.86	65.53	LLaVA-1.5	14.7	21.9	36.9	33.9	76.4	41.6	13.6
Ours	16.8	20.9	38.8	22.3	65.43	Ours	12.2	20.7	34.6	30.0	74.0	45.7	13.3

tions, ensuring that all spatial relations and layout elements are strictly text-faithful. As a result, the dataset provides a unified spatial supervision resource that supports spatial planning, spatial relation modeling, and rotation-based data augmentation within a single framework. The dataset will be publicly released.

5 Experiments

5.1 Experimental Setup

Training Protocol. We adopt a two-stage training protocol, in which Stage 1 optimizes only the text-to-image generation objective, whereas Stage 2 jointly optimizes both understanding and generation tasks.

Stage 1 (Generation Training). In the first stage, we freeze the MLLM and update only the Transformer connector and the diffusion backbone. The model is trained on Git10M [Liu *et al.*, 2025a], a large-scale remote sensing image–text corpus containing approximately 10 million pairs. This stage focuses on text-to-image generation, enabling the diffusion backbone to internalize the visual characteristics of overhead imagery, including top-down viewpoints and remote-sensing-specific textures, thereby establishing a robust generative prior.

Stage 2 (Joint Understanding–Generation Training). In the second stage, we unfreeze the remaining trainable components while keeping the MLLM visual encoder (ViT) and the diffusion VAE fixed. We jointly optimize multimodal understanding objectives—including VQA, captioning, and grounding—together with text-to-image generation. Training data in this stage include RSICap [Hu *et al.*, 2025], VRSBench [Li *et al.*, 2024], and the proposed RS-Spatial dataset. RSICap and VRSBench are used for multimodal understanding, with their captions reused as prompts for text-to-image generation, while RS-Spatial provides spatial layout plans, spatial relation labels, and rotation-consistent image–caption pairs to support spatial planning, spatial relation modeling, and geometry-consistent data augmentation. Note that for spatial layout plans, we apply them to both understanding and generation training, enabling the model to learn not only to produce layout plans from language inputs, but also to utilize these plans for image synthesis.

Implementation Details. All models are trained using the AdamW optimizer with a batch size of 1024 on 8 NVIDIA

A800 GPUs (80GB). Both training stages employ a cosine learning rate schedule with a 10% warmup phase. Stage 1 is trained for 10 epochs with an initial learning rate of 2×10^{-5} . Stage 2 is fine-tuned for 5 epochs with an initial learning rate of 1×10^{-5} . The balancing coefficient for the spatial supervision loss is set to $\lambda = 0.1$.

5.2 Comparison with SoTA Models

We compare Uni-RS with existing remote sensing text-to-image generation models on RSICD, RSIEval, and VRSBench.

Text-to-Image Generation on RSICD. Table 1 reports results on RSICD using FID, zero-shot classification accuracy (Cls-OA), and CLIP score. Following common practice in prior work, we report results under two settings: with RSICD fine-tuning, where Uni-RS is fine-tuned on the RSICD training set for five epochs before evaluation, and without RSICD fine-tuning. As shown in Table 1, fine-tuning Uni-RS on RSICD leads to state-of-the-art performance across all three metrics. Notably, even without RSICD fine-tuning, Uni-RS outperforms Text2Earth and several prior methods that are explicitly fine-tuned on RSICD, such as CRS-Diff [Tang *et al.*, 2024] and Txt2Img-MHN [Xu *et al.*, 2023]. These results demonstrate strong text-to-image generation capability and generalization of Uni-RS, consistent with prior findings that enhanced multimodal understanding can benefit generation performance [Deng *et al.*, 2025].

Spatial Faithful generation on RSIEval and VRSBench. Table 2 reports results on RSIEval and VRSBench. Compared to RSICD, captions in RSIEval and VRSBench are longer and more structured, typically involving multiple objects and explicitly specified spatial relations. These characteristics make spatial layout adherence a central factor in evaluating generation quality. For a fair comparison with the prior state-of-the-art model Text2Earth, we further fine-tune Text2Earth on VRSBench and RSICap for 5 epochs using the same training protocol.

As shown in Table 2, Uni-RS outperforms the fine-tuned Text2Earth model across all metrics on both benchmarks. On RSIEval, Uni-RS reduces FID by over 40% compared to the fine-tuned Text2Earth model, while improving the Spatially Faithful Rate (SFR) by approximately 25%. On VRSBench, Uni-RS achieves a reduction of over 40% in FID and an increase of approximately 2% in CLIP score. The pronounced

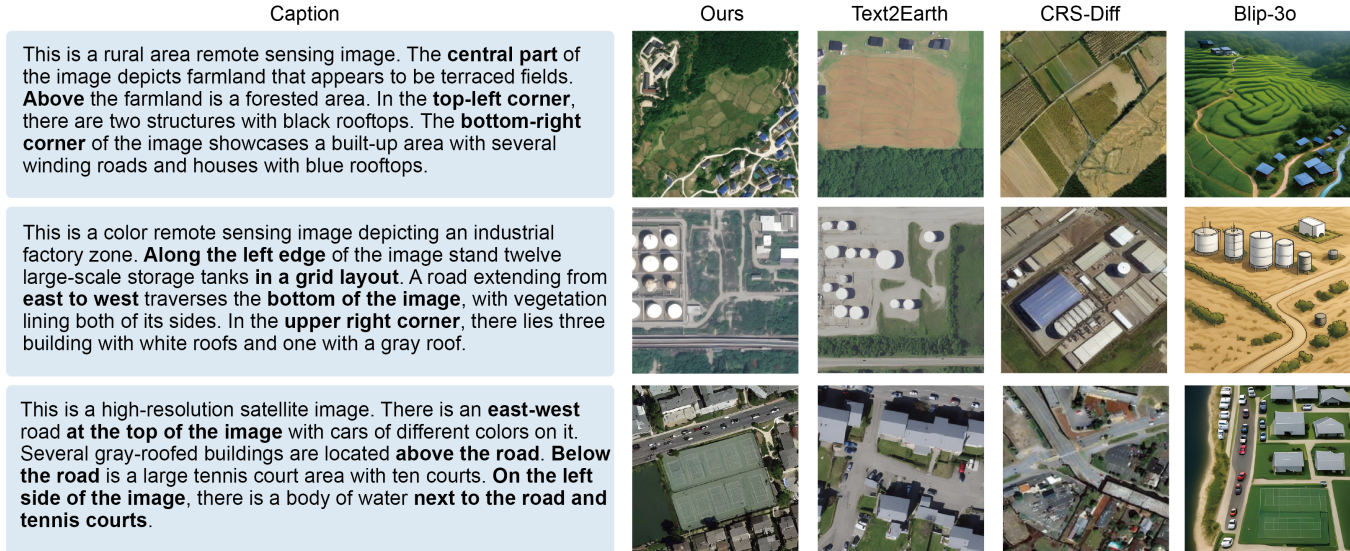


Figure 4: Qualitative comparison of spatial faithfulness in text-to-image generation. BLIP-3o is a general-domain unified multimodal model for understanding and generation, while CRS-Diff and Text2Earth are remote-sensing-specific text-to-image generation models. Text2Earth model is fine-tuned using RSIEval and VRSBench dataset to produce 512×512 images.

improvement in SFR indicates that Uni-RS is not only capable of generating the target objects, but also places them in accordance with the layout specified in the caption.

Understanding Tasks. Table 3 reports results on image captioning, visual question answering, and visual grounding tasks. Across all three tasks, Uni-RS achieves performance comparable to existing remote sensing vision–language models, with minimal performance gaps on the reported metrics. These results demonstrate that Uni-RS functions as an effective unified model, exhibiting strong multimodal understanding while simultaneously supporting text-to-image generation.

Qualitative Analysis As shown in Figure 4, qualitative results further corroborate the quantitative findings. General-domain unified models are able to correctly identify intended objects, while they often fail to generate overhead viewpoint. In contrast, remote-sensing-specific generation models produce images with more realistic overhead appearances, but frequently struggle to faithfully follow the objects and to place them in spatial configurations consistent with the described layouts. By comparison, Uni-RS is able to consistently synthesize the objects described in the caption while simultaneously respecting their intended spatial arrangements.

5.3 Ablation Study

We perform an ablation study to evaluate the contribution of each proposed component. Results are reported in Table 4 on RSIEval and VRSBench. Overall, the ablation results show that all three components consistently improve spatial faithfulness, and their effects accumulate in a stable and complementary manner. Introducing spatial layout planning already leads to a clear gain in spatially faithful generation, while simultaneously improving image fidelity and semantic alignment, as reflected by reduced FID and higher CLIP scores.

Table 4: Ablation study on VRSBench and RSIEval. Components are added cumulatively: (1) Spatial-Layout Planning (SLP), (2) Spatial-aware Query Supervision (SQS), (3) Image–Caption Spatial Layout Variation (ISV).

Method	VRSBench		RSIEval		
	FID	CLIP	FID	CLIP	SFR
Base	4.91	0.2533	13.47	0.2370	47.60
Base + SLP	4.62	0.2540	13.44	0.2381	54.00
Base + SLP + SQS	4.64	0.2542	13.33	0.2379	63.40
Base + SLP + SQS + ISV	4.51	0.2546	13.04	0.2401	80.15

Image–caption spatial layout transformation further strengthens this trend by exposing the model to geometry-consistent variations, yielding additional improvements in both spatial adherence and overall generation quality. In contrast, spatial-aware query supervision primarily enhances spatial faithfulness by reinforcing instruction-level spatial constraints in the conditioning space, while having only a marginal impact on FID and CLIP. When combined, the three components progressively mitigate the Spatial Reversal Curse, achieving the highest spatial fidelity across benchmarks without degrading generation quality.

6 Conclusion

We presented Uni-RS, the first unified remote sensing vision–language model that systematically investigates and mitigates the Spatial Reversal Curse between understanding and generation. By introducing spatially explicit mechanisms through Spatial-Layout Planning and incorporating spatial supervision for latent queries, Uni-RS improves spatial faithfulness in text-to-image generation while preserving strong multimodal understanding. Extensive experiments across multiple

benchmarks demonstrate that Uni-RS effectively integrates spatial understanding and spatial execution within a single unified framework.

References

[Bai *et al.*, 2025a] Shuai Bai, Yuxuan Cai, Ruizhe Chen, Keqin Chen, Xionghui Chen, Zesen Cheng, Lianghao Deng, Wei Ding, Chang Gao, Chunjiang Ge, Wenbin Ge, Zhifang Guo, Qidong Huang, Jie Huang, Fei Huang, Binyuan Hui, Shutong Jiang, Zhaohai Li, Mingsheng Li, Mei Li, Kaixin Li, Zicheng Lin, Junyang Lin, Xuejing Liu, Jiawei Liu, Chenglong Liu, Yang Liu, Dayiheng Liu, Shixuan Liu, Dunjie Lu, Ruilin Luo, Chenxu Lv, Rui Men, Lingchen Meng, Xuancheng Ren, Xingzhang Ren, Sibo Song, Yuchong Sun, Jun Tang, Jianhong Tu, Jianqiang Wan, Peng Wang, Pengfei Wang, Qiuyue Wang, Yuxuan Wang, Tianbao Xie, Yiheng Xu, Haiyang Xu, Jin Xu, Zhibo Yang, Mingkun Yang, Jianxin Yang, An Yang, Bowen Yu, Fei Zhang, Hang Zhang, Xi Zhang, Bo Zheng, Humen Zhong, Jingren Zhou, Fan Zhou, Jing Zhou, Yuanzhi Zhu, and Ke Zhu. Qwen3-vl technical report. *arXiv preprint arXiv:2511.21631*, 2025.

[Bai *et al.*, 2025b] Shuai Bai, Keqin Chen, Xuejing Liu, Jialin Wang, Wenbin Ge, Sibo Song, Kai Dang, Peng Wang, Shijie Wang, Jun Tang, Humen Zhong, Yuanzhi Zhu, Mingkun Yang, Zhaohai Li, Jianqiang Wan, Pengfei Wang, Wei Ding, Zheren Fu, Yiheng Xu, Jiabo Ye, Xi Zhang, Tianbao Xie, Zesen Cheng, Hang Zhang, Zhibo Yang, Haiyang Xu, and Junyang Lin. Qwen2.5-vl technical report. *arXiv preprint arXiv:2502.13923*, 2025.

[Berglund *et al.*, 2024] Lukas Berglund, Meg Tong, Maximilian Kaufmann, Mikita Balesni, Asa Cooper Stickland, Tomasz Korbak, and Owain Evans. The reversal curse: LLMs trained on “a is b” fail to learn “b is a”. In *The Twelfth International Conference on Learning Representations*, 2024.

[Chen *et al.*, 2025a] Juhai Chen, Zhiyang Xu, Xichen Pan, Yushi Hu, Can Qin, Tom Goldstein, Lifu Huang, Tianyi Zhou, Saining Xie, Silvio Savarese, et al. Blip3-o: A family of fully open unified multimodal models-architecture, training and dataset. *arXiv preprint arXiv:2505.09568*, 2025.

[Chen *et al.*, 2025b] Xiaokang Chen, Zhiyu Wu, Xingchao Liu, Zizheng Pan, Wen Liu, Zhenda Xie, Xingkai Yu, and Chong Ruan. Janus-pro: Unified multimodal understanding and generation with data and model scaling. *arXiv preprint arXiv:2501.17811*, 2025.

[Deng *et al.*, 2025] Chaorui Deng, Deyao Zhu, Kunchang Li, Chenhui Gou, Feng Li, Zeyu Wang, Shu Zhong, Weihao Yu, Xiaonan Nie, Ziang Song, Guang Shi, and Haoqi Fan. Emerging properties in unified multimodal pretraining. *arXiv preprint arXiv:2505.14683*, 2025.

[Fiaz *et al.*, 2025] Mustansar Fiaz, Hiyam Debary, Paolo Fraccaro, Danda Paudel, Luc Van Gool, Fahad Khan, and Salman Khan. Geovlm-r1: Reinforcement fine-tuning for improved remote sensing reasoning. *arXiv preprint arXiv:2509.25026*, 2025.

[Hu *et al.*, 2025] Yuan Hu, Jianlong Yuan, Congcong Wen, Xiaonan Lu, Yu Liu, and Xiang Li. Rsgpt: A remote sensing vision language model and benchmark. *ISPRS Journal of Photogrammetry and Remote Sensing*, 224:272–286, 2025.

[Khanna *et al.*, 2024] Samar Khanna, Patrick Liu, Linqi Zhou, Chenlin Meng, Robin Rombach, Marshall Burke, David B. Lobell, and Stefano Ermon. Diffusionsat: A generative foundation model for satellite imagery. In *The Twelfth International Conference on Learning Representations*, 2024.

[Kuckreja *et al.*, 2024] Kartik Kuckreja, Muhammad Sohail Danish, Muzammal Naseer, Abhijit Das, Salman Khan, and Fahad Shahbaz Khan. Geochat: Grounded large vision-language model for remote sensing. In *Proceedings of the IEEE/CVF Conference on Computer Vision and Pattern Recognition*, pages 27831–27840, 2024.

[Köksal and Alatan, 2025] Aybora Köksal and A. Aydin Alatan. Tinyrs-r1: Compact vision language model for remote sensing. *IEEE Geoscience and Remote Sensing Letters*, 22:1–5, 2025.

[Li *et al.*, 2024] Xiang Li, Jian Ding, and Mohamed Elhosiny. Vrsbench: A versatile vision-language benchmark dataset for remote sensing image understanding. *Advances in Neural Information Processing Systems*, 37:3229–3242, 2024.

[Li *et al.*, 2025] Kaiyu Li, Zepeng Xin, Li Pang, Chao Pang, Yupeng Deng, Jing Yao, Guisong Xia, Deyu Meng, Zhi Wang, and Xiangyong Cao. Segearth-r1: Geospatial pixel reasoning via large language model. *arXiv preprint arXiv:2504.09644*, 2025.

[Li *et al.*, 2026] Wenshuai Li, Xiantai Xiang, Zixiao Wen, Guangyao Zhou, Ben Niu, Feng Wang, Lijia Huang, Qiantong Wang, and Yuxin Hu. Georeason: Aligning thinking and answering in remote sensing vision-language models via logical consistency reinforcement learning. *arXiv preprint arXiv:2601.04118*, 2026.

[Liang *et al.*, 2025] Weixin Liang, LILI YU, Liang Luo, Srinivas Iyer, Ning Dong, Chunting Zhou, Gargi Ghosh, Mike Lewis, Luke Zettlemoyer, and Xi Victoria Lin. Mixture-of-transformers: A sparse and scalable architecture for multimodal foundation models. In *ICLR 2025 Workshop on Modularity for Collaborative, Decentralized, and Continual Deep Learning*, 2025.

[Liu *et al.*, 2023] Haotian Liu, Chunyuan Li, Qingyang Wu, and Yong Jae Lee. Visual instruction tuning. *Advances in neural information processing systems*, 36:34892–34916, 2023.

[Liu *et al.*, 2025a] Chenyang Liu, Keyan Chen, Rui Zhao, Zhengxia Zou, and Zhenwei Shi. Text2earth: Unlocking text-driven remote sensing image generation with a global-scale dataset and a foundation model. *IEEE Geoscience and Remote Sensing Magazine*, 2025.

[Liu *et al.*, 2025b] Jiaqi Liu, Lang Sun, Ronghao Fu, and Bo Yang. Towards faithful reasoning in remote

sensing: A perceptually-grounded geospatial chain-of-thought for vision-language models. *arXiv preprint arXiv:2509.22221*, 2025.

[Luo *et al.*, 2024] Junwei Luo, Zhen Pang, Yongjun Zhang, Tingzhu Wang, Linlin Wang, Bo Dang, Jiangwei Lao, Jian Wang, Jingdong Chen, Yihua Tan, et al. Skysensegpt: A fine-grained instruction tuning dataset and model for remote sensing vision-language understanding. *arXiv preprint arXiv:2406.10100*, 2024.

[Pan *et al.*, 2025] Xichen Pan, Satya Narayan Shukla, Aashu Singh, Zhuokai Zhao, Shlok Kumar Mishra, Jialiang Wang, Zhiyang Xu, Juhai Chen, Kunpeng Li, Felix Juefei-Xu, Ji Hou, and Saining Xie. Transfer between modalities with metaqueries. *arXiv preprint arXiv:2504.06256*, 2025.

[Tang *et al.*, 2024] Datao Tang, Xiangyong Cao, Xingsong Hou, Zhongyuan Jiang, Junmin Liu, and Deyu Meng. Crs-diff: Controllable remote sensing image generation with diffusion model. *IEEE Transactions on Geoscience and Remote Sensing*, 2024.

[Team, 2024] Chameleon Team. Chameleon: Mixed-modal early-fusion foundation models. *arXiv preprint arXiv:2405.09818*, 2024.

[Wang *et al.*, 2024] Xinlong Wang, Xiaosong Zhang, Zhengxiong Luo, Quan Sun, Yufeng Cui, Jinsheng Wang, Fan Zhang, Yueze Wang, Zhen Li, Qiying Yu, et al. Emu3: Next-token prediction is all you need. *arXiv preprint arXiv:2409.18869*, 2024.

[Wang *et al.*, 2025a] Di Wang, Shunyu Liu, Wentao Jiang, Fengxiang Wang, Yi Liu, Xiaolei Qin, Zhiming Luo, Chaoyang Zhou, Haonan Guo, Jing Zhang, et al. Geozero: Incentivizing reasoning from scratch on geospatial scenes. *arXiv preprint arXiv:2511.22645*, 2025.

[Wang *et al.*, 2025b] Fengxiang Wang, Mingshuo Chen, Yueying Li, Di Wang, Haotian Wang, Zonghao Guo, Zefan Wang, Shan Boqi, Long Lan, Yulin Wang, Hongzhen Wang, Wenjing Yang, Bo Du, and Jing Zhang. GeоЛLaVA-8k: Scaling remote-sensing multimodal large language models to 8k resolution. In *The Thirty-ninth Annual Conference on Neural Information Processing Systems*, 2025.

[Wei *et al.*, 2022] Jason Wei, Xuezhi Wang, Dale Schuurmans, Maarten Bosma, Fei Xia, Ed Chi, Quoc V Le, Denny Zhou, et al. Chain-of-thought prompting elicits reasoning in large language models. *Advances in neural information processing systems*, 35:24824–24837, 2022.

[Wu *et al.*, 2025] Chenfei Wu, Jiahao Li, Jingren Zhou, Junyang Lin, Kaiyuan Gao, Kun Yan, Sheng-ming Yin, Shuai Bai, Xiao Xu, Yilei Chen, et al. Qwen-image technical report. *arXiv preprint arXiv:2508.02324*, 2025.

[Xia *et al.*, 2018] Gui-Song Xia, Xiang Bai, Jian Ding, Zhen Zhu, Serge Belongie, Jiebo Luo, Mihai Datcu, Marcello Pelillo, and Liangpei Zhang. Dota: A large-scale dataset for object detection in aerial images. In *Proceedings of the IEEE conference on computer vision and pattern recognition*, pages 3974–3983, 2018.

[Xie *et al.*, 2024] Enze Xie, Junsong Chen, Junyu Chen, Han Cai, Haotian Tang, Yujun Lin, Zhekai Zhang, Muyang Li, Ligeng Zhu, Yao Lu, et al. Sana: Efficient high-resolution image synthesis with linear diffusion transformers. *arXiv preprint arXiv:2410.10629*, 2024.

[Xie *et al.*, 2025] Jinheng Xie, Weijia Mao, Zechen Bai, David Junhao Zhang, Weihao Wang, Kevin Qinghong Lin, Yuchao Gu, Zhijie Chen, Zhenheng Yang, and Mike Zheng Shou. Show-o: One single transformer to unify multimodal understanding and generation. In *The Thirteenth International Conference on Learning Representations*, 2025.

[Xu *et al.*, 2023] Yonghao Xu, Weikang Yu, Pedram Ghamisi, Michael Kopp, and Sepp Hochreiter. Txt2img-mhn: Remote sensing image generation from text using modern hopfield networks. *IEEE Transactions on Image Processing*, 32:5737–5750, 2023.

[Yang *et al.*, 2025] Yueguang Yang, Jiahui Qu, Ling Huang, and Wenqian Dong. Dpmamba: distillation prompt mamba for multimodal remote sensing image classification with missing modalities. In *Proceedings of the Thirty-Fourth International Joint Conference on Artificial Intelligence, IJCAI '25*, 2025.

[Yerramilli *et al.*, 2025] Sahiti Yerramilli, Nilay Pande, Ryanaa Grover, and Jayant Sravan Tamarapalli. GeoChain: Multimodal Chain-of-Thought for Geographic Reasoning, September 2025.

[Yu *et al.*, 2024] Zhiping Yu, Chenyang Liu, Liqin Liu, Zhenwei Shi, and Zhengxia Zou. Metaearth: A generative foundation model for global-scale remote sensing image generation. *IEEE Transactions on Pattern Analysis and Machine Intelligence*, 2024.

[Zhang *et al.*, 2024a] Wei Zhang, Miaoxin Cai, Tong Zhang, Yin Zhuang, and Xuerui Mao. Earthgpt: A universal multi-modal large language model for multi-sensor image comprehension in remote sensing domain. *IEEE Transactions on Geoscience and Remote Sensing*, 2024.

[Zhang *et al.*, 2024b] Zhuosheng Zhang, Aston Zhang, Mu Li, hai zhao, George Karypis, and Alex Smola. Multimodal chain-of-thought reasoning in language models. *Transactions on Machine Learning Research*, 2024.

[Zhang *et al.*, 2025] Xinjie Zhang, Jintao Guo, Shanshan Zhao, Minghao Fu, Lunhao Duan, Jiakui Hu, Yong Xien Chng, Guo-Hua Wang, Qing-Guo Chen, Zhao Xu, et al. Unified multimodal understanding and generation models: Advances, challenges, and opportunities. *arXiv preprint arXiv:2505.02567*, 2025.

[Zhao and Shi, 2021] Rui Zhao and Zhenwei Shi. Text-to-remote-sensing-image generation with structured generative adversarial networks. *IEEE Geoscience and Remote Sensing Letters*, 19:1–5, 2021.

[Zhou *et al.*, 2024] Chunting Zhou, Lili Yu, Arun Babu, Kushal Tirumala, Michihiro Yasunaga, Leonid Shamis, Jacob Kahn, Xuezhe Ma, Luke Zettlemoyer, and Omer Levy. Transfusion: Predict the next token and diffuse

images with one multi-modal model. *arXiv preprint arXiv:2408.11039*, 2024.